Frontiers in Nanoscience and Nanotechnology

Research Article ISSN: 2397-6527

Validation of copper decorated Graphene oxide material for assaying Curcumin

Nibedita Dey[1], Devasena T[2*] and Rama Shanker Verma[3*]

[1]Saveetha School of Engineering, Saveetha Institute of Medical and Technical Sciences, Saveetha University, Thandalam, India

[2]Centre for Nanoscience and Technology, Anna University, Chennai – 600025, India

[3]Stem Cell and Molecular biology Laboratory, Department of Biotechnology, Indian Institute of Technology Madras, Chennai-600036 Tamil Nadu, India

Abstract

Sensing has found its own place in the field of research. Novel and innovative ways to sense compounds have always been of great interest in the field of interdisciplinary sciences. The major problems observed with this wonder drug in stable in aqueous environment. This attributes to very minimum amount of this therapeutic in tissues and plasma. But artificial increase in curcumin concentration through supplements could have an inverse effect on the human body. As an alternative it is been commercially utilized all around the world as a dietary supplement. But, with the increased consumption of curcumin its toxicity level tends to rise in the systemic circulation. So, an alternate, fast, economical way of sensing curcumin is essential. Among all the detection systems electrochemical workstation is standing at the forefront for easy and efficient detection. we have attempted to utilize cyclic voltammetry mode for detection of our target. Three modified electrodes of Glassy Carbon electrode (GCE) were analysed - Copper, Copper-Graphene oxide (Cu-GO) modified electrode and Copper- reduced graphene oxide (Cu-rGO) modified electrode of which Cu-GO modified electrode showed better signal quality and lower detection limit than Cu-rGO modified electrode. The detection limit was found to be 4.7 nM and 0.02 nM for Cu-GO and Cu-rGO electrode respectively. The electrodes showed good reproducibility, good selectivity and a potential platform for sensing numerous compounds in future.

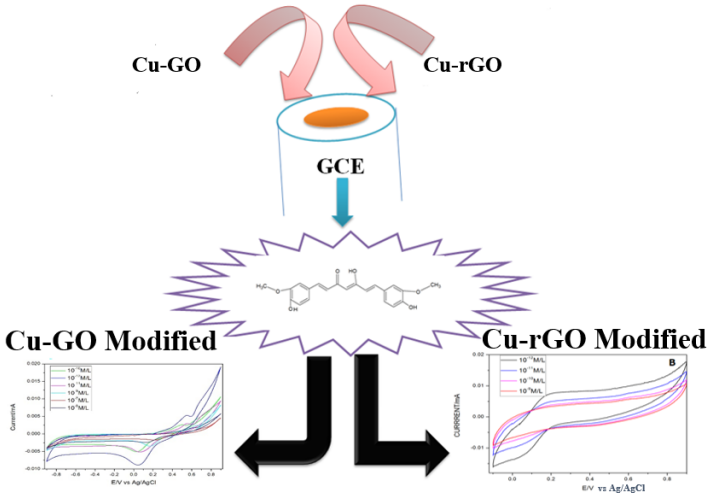

Graphical Interpretation of Graphene oxide material

Introduction

Sp2 hybridized carbon sheets packed in honeycomb lattices, graphene and its oxide forms possess enhanced surface area and properties [1,2]. Composites of the same with metal nanoparticles are drawing attention to form atom thick three-dimensional hybrids with unique properties [3-5]. Studies have shown that these carbon matrixes can be prevented from aggregation and maintain the sheet properties by incorporating inorganic nanoparticles [6-10]. Down the years various metal oxide–graphene nanocomposites for specific applications involve iron, manganese, cobalt, zinc, tin, etc. [11-

Correspondence to: Devasena T,Professor, Centre for Nanoscience and Technology, ACT campus, Anna University, Chennai-600025, India, E-mail: tdevasenabio@gmail.com

Verma RS, Prof., Head, Stem cell and Molecular Biology Laboratory, Bhupat and Jyoti Mehta school of Biosciences, Department of Biotechnology, IIT-Madras Chennai-600036, Tamil Nadu, India, Tel: 044 2257 4109; Email: vermars@iitm.ac.in

Key words: *copper- graphene oxide modified electrode, copper reduced graphene oxide modified electrode, cyclic voltammtery, curcumin*

Received: July 03, 2021; **Accepted:** October 05, 2021; **Published:** October 08, 2021

20]. Copper among all other nanoparticles has wide applications in electrochemical sensors [21-24]. So, decoration of copper metal was very much feasible to check the separate sensing effects of this marvel metal on GO and rGO (reduced graphene oxide).

Curcumin also called 1,7-bis- (4-hydroxy-3-methoxyphenyl)-1,6-heptadiene-3,5-dione) is a component of a valuable perennial herb named Curcuma longa. It is a dietary supplement whose major components are three curcuminoids. It has a characteristic yellow colour which gives it colourant property [25]. When it comes to its medicinal values it extends from antimicrobial, antiviral, antitumoral, antioxidant, antihyperlipidemic to antihepatotoxic, anti-Alzheimer's disease and anti-inflammatory. Hence, commonly known as 'multi anti-spice' or 'curecumin' in herbal medicine [26]. But this remarkable drug has its own drawbacks like insolubility in water, rapid metabolism, poor absorption and systemic elimination leading to limited bioavailability [27]. So, increase its bioavailability many novel and promising alternatives have opted like piperine, cyclodextrin encapsulation, ceramic and nanoparticle utilization, etc. [28,29]. These natural β-diketone ligands are ideal for chelating with a variety of metals to form complexes of medicinal value. The sterical structure of this drug is such that β-diketone at the centre is flanked by unsaturated phenolic groups which results in unusually flat β- ketone moieties. Thus, the overall conformation looks like that of an eagle with two large wings of flat β- ketone. The phenolic groups present in curcumin form additional centres of reactivity to form a complex with a metal [30].

This medicinal compound through human clinical trials has shown that its consumption is safe up to 12gms per day. Even the side effects seem to be very few. This compound has been considered safe by the United States food and drug administration department in the food industry. Oral ingestion of curcumin gets transformed into two major metabolites curcumin O- glucuronide (COG) and curcumin O-sulphate (COS) in all life forms. Other minor metabolites are Hexahydro curcumin and its curcuminol and glucuronide forms [31,32]. The major problems observed with this wonder drug in stable in aqueous environment. This attributes to very minimum amount of this therapeutic in tissues and plasma. For example, an oral dosage of curcumin up to 0.1g/kg in mice yields only 2.25 μg/mL of free plasma curcumin [33]. This decrease in bioavailability is due to poor solubility in an aqueous solution like water, minimum absorption in the intestine, systemic elimination and faster assimilation and excretion by hepatic organ. In a study to evaluate the pharmacokinetics of orally administered curcumin through HPLC, researchers found only one out of 12 healthy human volunteers had free curcumin in his plasma at a given time of the assay. That's the severity of the lack of bioavailability of curcumin. Even if 10-12g of curcumin is consumed as a single dose in a day it will only generate its glucuronide and sulphate forms. The literature states that there is no evidence of mixed conjugates in the plasma. So, taking high dosages could lead to increase absorption, but the biotransformation might reduce the presence of free active curcumin as it could be travelling to other sites other than the intestine [34].

This issue of non- bioavailability is tackled by the western countries by introduction of supplements of curcumin through daily diet. But, artificial increase in curcumin concentration through supplements could have an inverse effect on the human body as suggested by few studies. As the concentration of curcumin increases it not only will increase its efficiency but also toxicity. Human osteoblast cell lines undergo apoptotic changes at concentration lower than 25μM and at 50-200 μM necrotic cell death was triggered by curcumin [35]. One of the major absorption factors pieridine used in curcumin supplement should be consumed cautiously as it is inhibitor for few drugs. So, people consuming additional medications along with these supplements should know the consequences of the same [36,37]. Curcumin also causes anaemia in people with sub-optimal iron intake [38]. Enzymes that metabolize certain drugs namely glutathione-S-transferase, P450, UDP- glucuronosyltransferase etc. are hindered by curcumin that will lead to unmetabolized drugs in the plasma hence increasing the toxicity [39,40]. Gastric discomfort, diarrhoea, skin rashes, nausea, constipation, anti- platelet property, gall bladder contractions etc. are some of the negative effects of curcumin high dosage. So, patients having gall stones or on blood thinner need to be cautious with the amount of curcumin intake they take. Hence, these data facts gave us the insights to come up with a possible alternate, fast, economical way of sensing curcumin.

When it comes to electrode modifiers transition metal ions belonging to the first row like copper, nickel, cobalt, etc. have played a crucial role so far for both environmental and biological applications [41-43]. The bioavailability of curcumin apart from using additives, phospholipids, etc. can also be increased using metal ions and nanoparticles. These complexes of curcumin not only provide innovative and promising approaches to the drawbacks faced by curcumin researchers, but also lay platform for potential medicinal benefits of the same. These natural and rare β-diketones ideally chelate with a variety of metals and form stable complexes. Over the decades curcumin metal complexes have majorly excelled in the fields of neuroprotective effects, anticancer, antioxidant and anti-Alzheimer's properties. Among the major metal complexes of medicinal origin with copper, Vanadyl and copper followed by zinc have been studied extensively so far. So, our metal of interest turned out to be copper depending on the availability, cost and literature evidence. Copper complex with curcumin (Cu- curcumin) has possible anti- Alzheimer's property. Its mode of action is believed to be using Ab-aggregation blockers, Reactive Oxygen Species (ROS) and chelating ions [44]. This medicinal property of Cu-curcumin complex was flipped in the present study to see if a sensing system is possible using the same complex.

Among the different modes present in electrochemical workstation cyclic voltammetry is the most common mode. Exclusive use of this mode for detection has not been done before. For less viscous aqueous medium with lighter analytes Differential pulse voltammetry (DPV) or Linear sweep voltammetry (LSV) works well. This is because in these systems the sampling assay time is very fast and the double layer formed gets decayed rapidly. But, if the analyte has polar properties, have exceptionally strong forces of interaction with the supporting electrolyte which might be viscous in nature and is large in size then tables might turn. In these scenarios the capacitance layer is formed slowly and in large magnitude in DPV or SWV mode. So, CV works better in these conditions. It would apply potentials continuously for a long time, which would deplete the capacitance double layer. So, keeping these aspects into consideration we devised our present study to detect curcumin using cyclic voltammetry exclusively.

Materials and methods

All the materials required for the production of the GO and rGO have been used based on our previously published work [45]. Copper (II) sulphate pentahydrate, starch solution, ascorbic acid, sodium hydroxide and absolute alcohol were purchased from sigma Aldrich and used for synthesis of copper nanoparticles. Copper chloride, Nafion were used for UV-Vis studies and Cyclic voltammetry studies respectively. Sodium chloride (NaCl), potassium chloride (KCl),

sodium dihydrogen phosphate (NaH2PO4) and disodium hydrogen phosphate (Na2HPO4) were used to prepare the supporting electrolyte solution (pH 7.4). Fetal calf serum was purchased from Sigma Aldrich for checking analytical applications. Characterization were performed for the produced nanoparticles using XRD (CuKα), SEM (TESCAN VEGA3 SBU), UV-Vis spectrophotometer (UV-1800 SHIMADZU) and electrochemical studies (CH Instruments). The parameters and the electrodes systems were optimized and setup based on out previously published article [46].

Synthesis of copper nanoparticles

0.1M of copper (II) sulphate pentahydrate and 1.2% of starch solution were stirred continuously for 30 minutes. Then 50ml of (0.2M) ascorbic acid was added to the mixture and stirred for 30minutes. 30 ml of (1M) sodium hydroxide solution was allowed to stir continuously for 2 hours at 80°C then washed with water, ethanol and dried in vacuum desiccators overnight [47,48].

UV spectral studies

Solutions used for the analysis were 0.062 M of copper chloride solution; 0.0005 M Curcumin solution (0.0005M) and 1ml each of the above samples were mixed for the metal complex solution.

Results

The basic characterisation of the synthesized GO and rGO sheets can be referred from supplementary notes attached. The formation of GO and rGO powder was confirmed by XRD as depicted in Figure S1A. This is due to strong intercalation of oxygen groups in the GO and for rGO due to the π-π interaction of Carbon molecules. The broadness of the observed peak of rGO is due to the deoxygenation of GO to form sp2 hybridized carbon system [46]. The crystal structure and size of the synthesized copper were verified by XRD as shown in Figure 1B. They exhibited characteristic peaks at 43°, 51° and 74° with FCC structure [47]. To study the surface morphology of synthesized materials SEM was used. This demonstrated that the nanoparticles formed clusters. Starch was the effective stabilizing agent used in the present study for the fabrication of small-sized particles. The size was found to be on average around 200-250 nm. The average crystallite size of the synthesized copper nanoparticles calculated using Scherrer formula were found to be 244nm. This size is very much in range with our SEM results [47].

Copper was incorporated in GO and rGO via sonication for 1 hour in ethanol. SEM as shown in Figure 1C and 1D illustrated random crumpled sheets of GO and rGO. Henceforth we have named these coppers decorated GO and rGO sheets as Cu-GO and Cu-rGO for better understanding the further studies with the target. The SEM images of drug(curcumin) with Cu-GO and Cu-rGO are depicted in Figure 1 (B&D) respectively. Our main objective was to analyse the sensing aspect of the detector material hence only preliminary studies were performed for basic confirmation of the components in the detector material. Compared to the data produced by researchers with similar preliminary results have shown TEM results with copper embedded in the sheets and visible uncovered surfaces of Graphene. This results in a bumpy morphology. When sonicated initial deposition might occur at the edges followed the surface [46]. This coincides with the SEM images we obtained while study. (Figure 1)

The decoration of copper nanoparticles onto the GO sheets showed shift in the XRD peak which might be due to the reduction of GO to rGO by copper metal. This has been depicted by blue line in Figure 2A-2D. In rGO sheets, copper seemed to have been placed on the surface as the red XRD peak of rGO shows a small peak at 43° which coincides with coppers peak.

To check the interaction of our drug with copper, UV studies were recorded at 0 hour and after 48hours (Figure 2E). These studies initially showed a strong characteristic absorption peak at 400-440

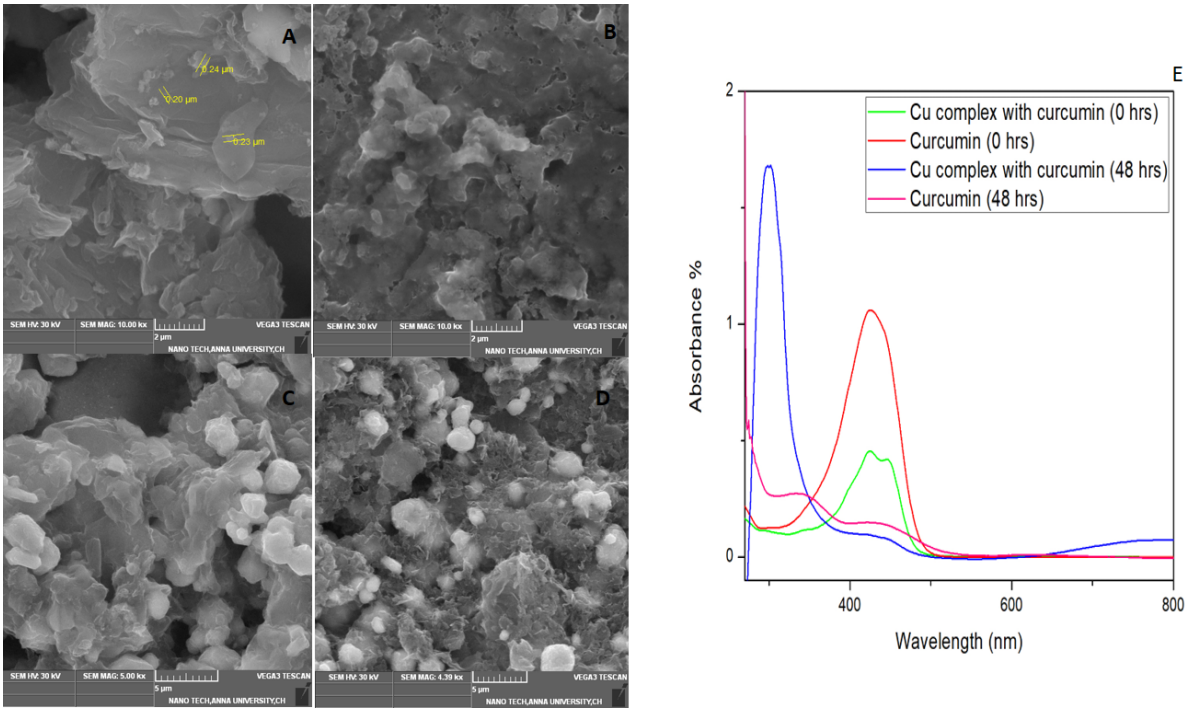

Figure 1. (A-D) SEM images of synthesized Cu-GO (scale 2 μm), Cu-GO with Curcumin (scale 2 μm), Cu-rGO (scale 5 μm) and Cu-GO (scale 5 μm) with Curcumin respectively. (1E) UV-Vis spectral studies on curcumin with copper

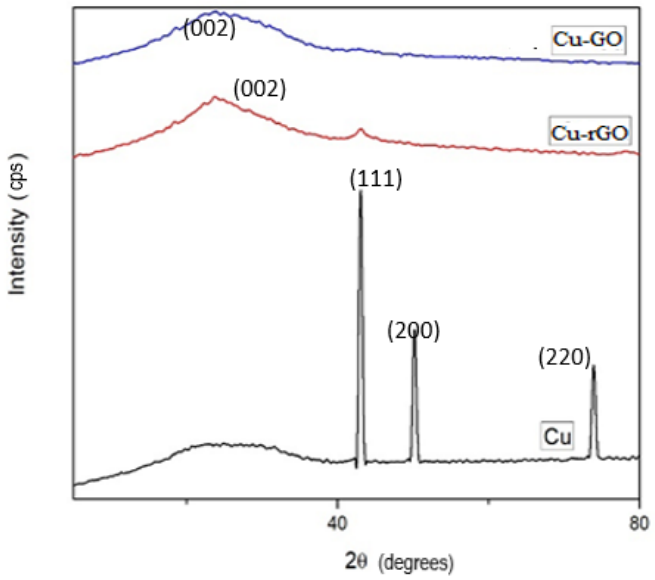

Figure 2. XRD for Cu-GO and Cu-rGO sheets

nm for curcumin (0 hours). This might be inferred to the band π → π* of the drug [48,49]. After 48 hours, both curcumin and its complex with copper manifested blue shift around 300 nm with a reduction in the peak. The blue shift and increase in intensity seen in the metal complex might be due to drug metal charge transfer or chelation with metal via β-diketone of the drug. Hence, we were able to infer that our drug formed a stable complex with the metal, which lasted even after 48 hours. This confirms the affinity of curcumin towards copper, further justifying the use of copper in the present study for sensing electrochemically [50]. Literature already reported that copper ions entrapped in drug interact with fibrils stay electrochemically active [51]. So, we were able to note that chelation of Curcumin with a few divalent metals could also be used for effective electrochemical sensing as they have previously contributed to potential medical applications. The 1:1 type chelation for curcumin with copper was used in the present study. This is by virtue of the complex's flexible orthorhombic geometry which keeps its antioxidant property active, hence electrochemically active. Even though o-methoxy phenolic groups and β-diketone cause chelation, but mostly it's the later [52-54].

The AFM images of Cu modified GO and rGO sheets are depicted in Figure 3A and 3B. Copper has been deposited up to a thickness of 800nm for both the carbon substrates. Figure 3C depicts the functionalization of GO and rGO sheets with Cu nanoparticles. Among the four concentrations used the lowest concentration of 250μL of copper was optimized to be the sensing quantity. This is due to similar functionalization seen in all the four concentrations of copper with the carbon sheets was found too similar. The lowest of concentrations gives apt functionalization of sheets as the highest concentration. Hence, we choose the lowest concentration (250μL) as the metal concentration to functionalize the sheets because use of lesser metal species will provide enough reaction space with our bulk target and also it would be economical to use lesser number of reactants. The native peak of copper shows a predominant O-H peak at 3250 cm^{-1} which infers that our copper nanoparticles have oxygen attached to it. This represents hydroxyl stretching vibrations on the surface of the nanoparticles. When compared with GO and rGO sheets we find 1624 cm^{-1} coinciding with the parent copper's FTIR peak [55]. Hence, we would like to infer the presence of copper in its oxide form on the surface of GO/rGO sheets.

Our primary aim was to find an alternate sensing method for curcumin. Hence, we limited our studies to preliminary analysis of the sensing materials to just confirm that the synthesized materials are Cu-GO and Cu-rGO. Material science aspect of it was not looked into in detail because of the same reason.

Sensing Assay

Before the modified electrodes were studied for their sensing ability, bare GCE studies were done with curcumin. This bare system showed reversible and diffusion limited redox electron transfer process. This has been depicted in Figure 4. There is no exhibition of redox peaks by GCE in PBS but with curcumin peak produces oxidation peaks at 0.2 V and 0.45 V. This is due to the formation of quinone and hydroquinone/quinone couple at 0.45 V and 0.2 V respectively. Curcumin forms a polymerization layer on the bare GCE surface upon continuous application of voltage which is assigned due the electrode's surface roughness and active reaction sites for transfer of electrons. Hence, this could also be stated as a two-electron two proton coupled process. As the electrode is used continuously curcumin deposits on GCE resulting in decrease in current flow [56,57]. Functional groups of GCE undergo nucleophilic reaction with o-quinone and 3,5 dione group of curcumin to form new bonds. (Figure 4).

Bare copper decorated GCE, was studied first to know the native electrochemical properties of the metal before incorporating it in GO or rGO. This setup showed an anodic peak appears at 0.16V and cathodic peak at -0.56V. This corresponds to the oxidation and reduction peaks of the metallic copper at the electrode in the concerned electrolyte. When curcumin (10-12 M/L) was added to the electrolyte and voltage was applied, it exhibited two oxidation peaks 0.09V (peak 1) and 0.54V (peak 2) and a reduction peak at -0.61V (Figure 5A). Figure 5B-5E illustrates the current patterns produced with an increase in drug concentration. The initial oxidation peak increases while the later decreases with increasing curcumin concentration (10-12 to 10-8 M/L). A graph was plotted with increasing scan rates and a current produced by the drug at 10-12M/L. The linear variation of scan rate was observed only in peak 1 (Figure 5D). The linear regression for peak 1 was found to be 0.91, S. D=0.00082 and N=7. Although the increase in the background current might be due to the modification of the electrodes but this increase varied from each material that we have used. And based on the literature we followed we found a current density plot with voltage was not needed [57]. Apart from that for a diffusion-control reaction the concentration of active species at the electrode-solution interface is time dependent, so increasing the scan rate will result in limiting current density increase. Hence current was chosen in one of the axis not current density for our study.

Cyclic Voltammetry studies were taken at physiological pH (7.4) for potential real-time applications. We have also attempted to study the lowest concentration possible with continues usage in this sensor. For longer usage, the copper decorated electrode showed reversible electron transfer with diffusion-limited redox process (Figure 6A-6D). With the increase in voltage, curcumin polymerizes and gets deposited onto the electrode surface. The peak 1 (0.09V) might attributes to the copper complex's peak with the drug, as it lies in close proximity to the bare copper's oxidation peak. The reaction with the drug might have caused the increase in current and shift in oxidation peak. The second peak (0.54V) is suggested to be the oxidation of the drug as per literature, because of the quinone derivative formation and quinone/hydroquinone redox couple respectively. Upon continuous runs with

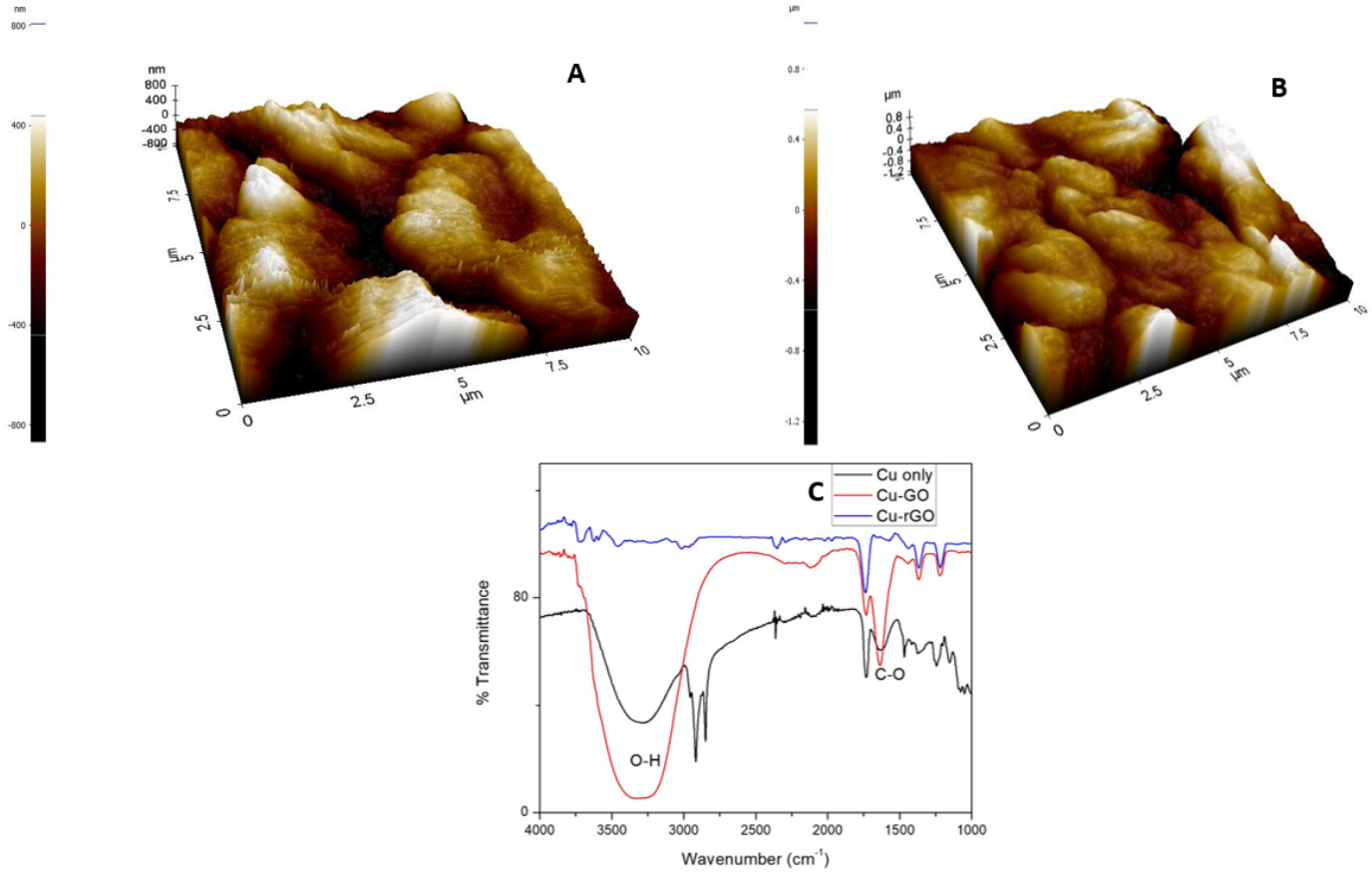

Figure 3. (A) AFM image of Cu-GO, (B) AFM image of Cu-rGO, (C) FTIR image of Cu, Cu-GO and Cu-rGO

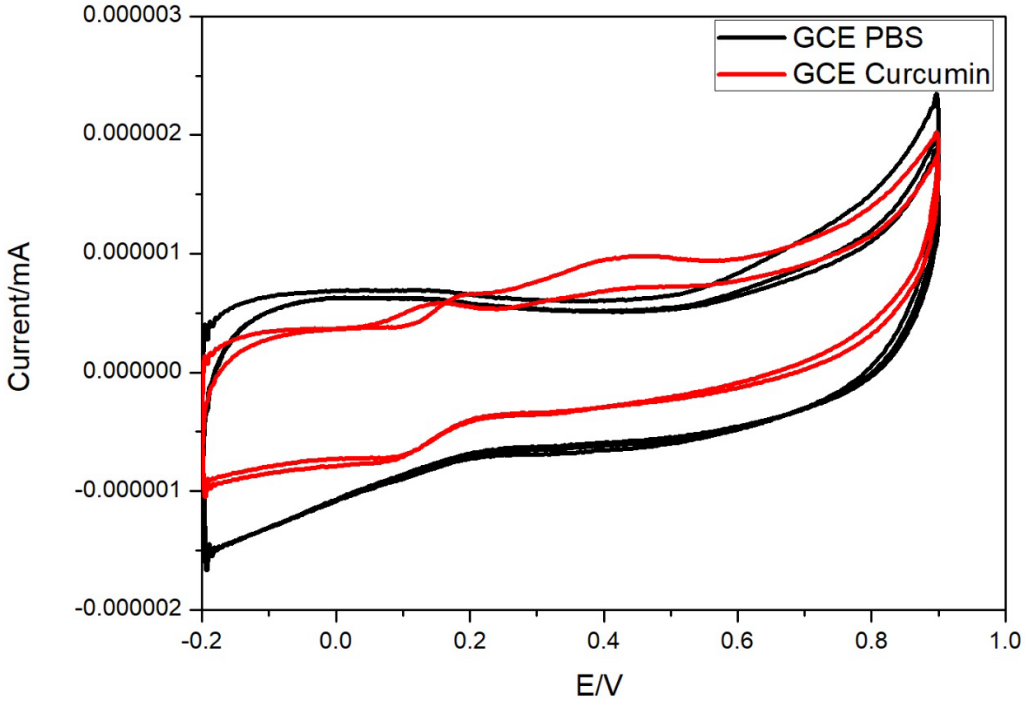

Figure 4. Cyclic voltammograms of curcumin at GCE electrode with and without curcumin.

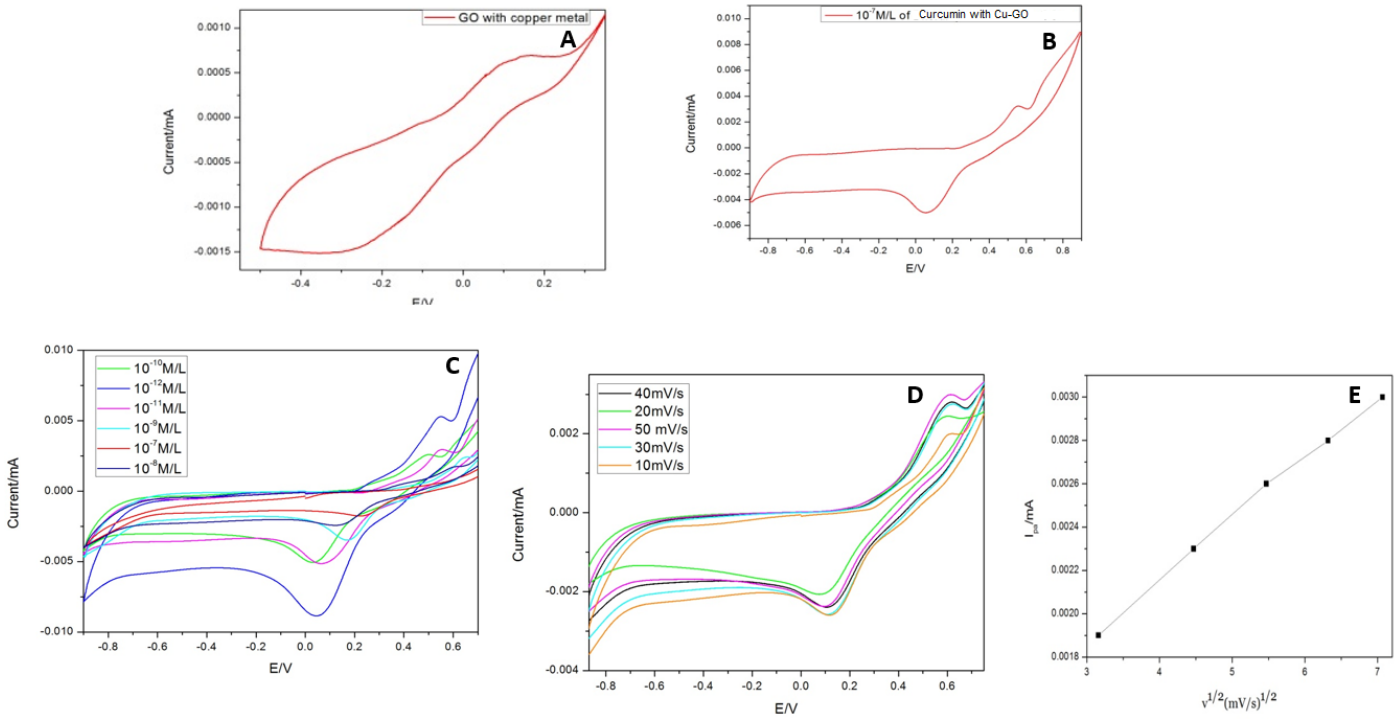

Figure 5. (A) CV studies of Cu-GO. (B) CV studies of Cu-GO with curcumin. (C) CV studies of Cu-GO with different concentrations of curcumin. (D) CV studies of Cu-GO at different scan. (E) Linear variation of scan rate with current for Cu-GO modified electrode

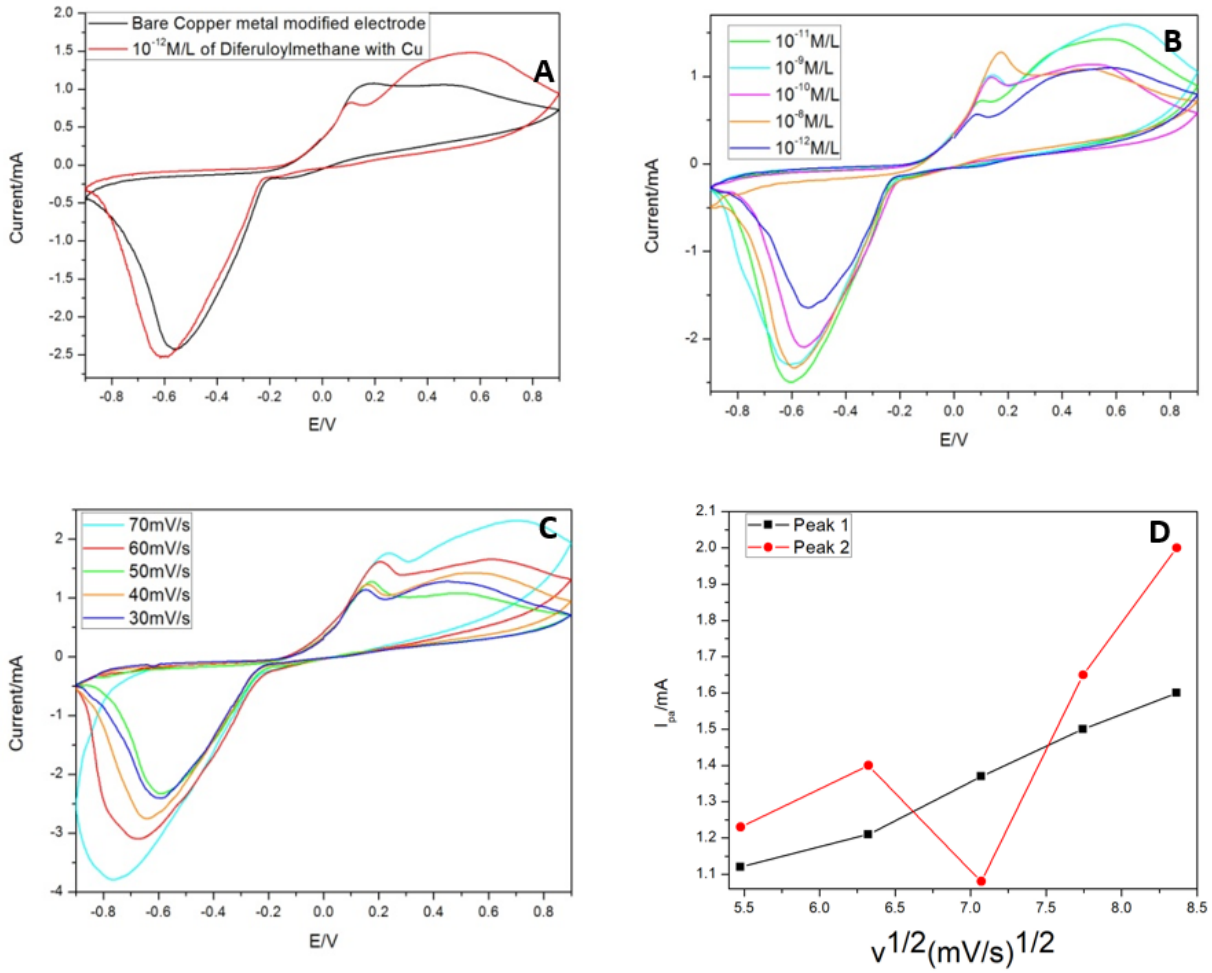

Figure 6. (A): CV studies of Cu with and without curcumin. (B) CV studies of Cu for different concentrations of Curcumin. (C) CV studies of Cu at different scans. (D) Linear variation of CV studies of Cu with scan rate and current

an increase in concentrations, the current density increases for peak 1 and decreases in peak 2 (Figure 6B). The decrease can be attributed to the deposition on the reaction surface of the working electrode [58,59]. While the increase in current with an increase in concentration is due to the increased metal chelation with the drug and forming active electroactive species. The o-quinone group and 3,5 dione group in the drug undergo nucleophilic reaction with metal causing coordination bond formation. With increasing, scan rates peak 1 shows an increase in the current while the other peak follows a zig-zag pattern (Figure 6C and 6D). The continuous deposition of curcumin at the surface might hinder the charge transfer at the surface. While the complex with metal enhances the charge transfer. So, peak 1 was considered for sensitivity assay in the further studies.

Sensing using Cu-GO and Cu-rGO electrodes

With copper decorated at the GO and rGO surface, there has been an increase in the electro-active nature of the modified electrodes. Figure 5A and 5B depicts Cu-GO with oxidation peak at +0.12V and reduction peak at -0.2V for bare electrolyte and 0.54V and -0.06V in the supporting electrolyte containing curcumin (10-12 M/L). Similarly, Figure 7 shows the change in current in PBS using Cu-GO modified electrode for different concentrations of our target material. The concentrations were based on our previously reported data [46]. The change in current with scan rate and linear variation of scan rate for Cu-GO is illustrated in Figure 5D and 5E. The linear regression for peak of Cu-GO was calculated to be 0.997 with standard deviation of 0.0022.

Cu-rGO shows oxidation peak at +0.13V and reduction peak at -0.003V in PBS. When curcumin was added to the supporting electrolyte the current decreased drastically with a light oxidation peak at 0.6V and negligible reduction peak. This shows that it is not a reversible reaction (Figure 7A). Figure 7B and 7C shows the change in current in for Cu-rGO at different amounts of the target compound and at different scan rates respectively. The change in current with scan rate and linear variation of scan rate with current for Cu-rGO is illustrated in Figure 7D. The linear regression for the peak of Cu-rGO was found to be 0.9 with standard deviation of 0.0022 for 7 cycles.

For Cu-GO modified electrode with oxidation peak is almost similar to that of the bare metal at 0.12V, hence proving the presence of participation the metal in the redox reaction. But the reduction peak has shifted considerably due to the incorporation in GO. On addition of curcumin the oxidation peak falls again at 0.54V which makes us infer that the drugs oxidation peak has negligible change when the main detection material is GO in an electrochemical workstation. For increase in concentration of the target, the current decreases as the drug gets deposited during continuous runs. Hence, limiting the number of cycles runs for this electrode. Linear variation of scan rate with current illustrated in Figure 7D and 7E shows that diffusion-based reaction takes place at electrode surface. Cu-rGO modified electrode

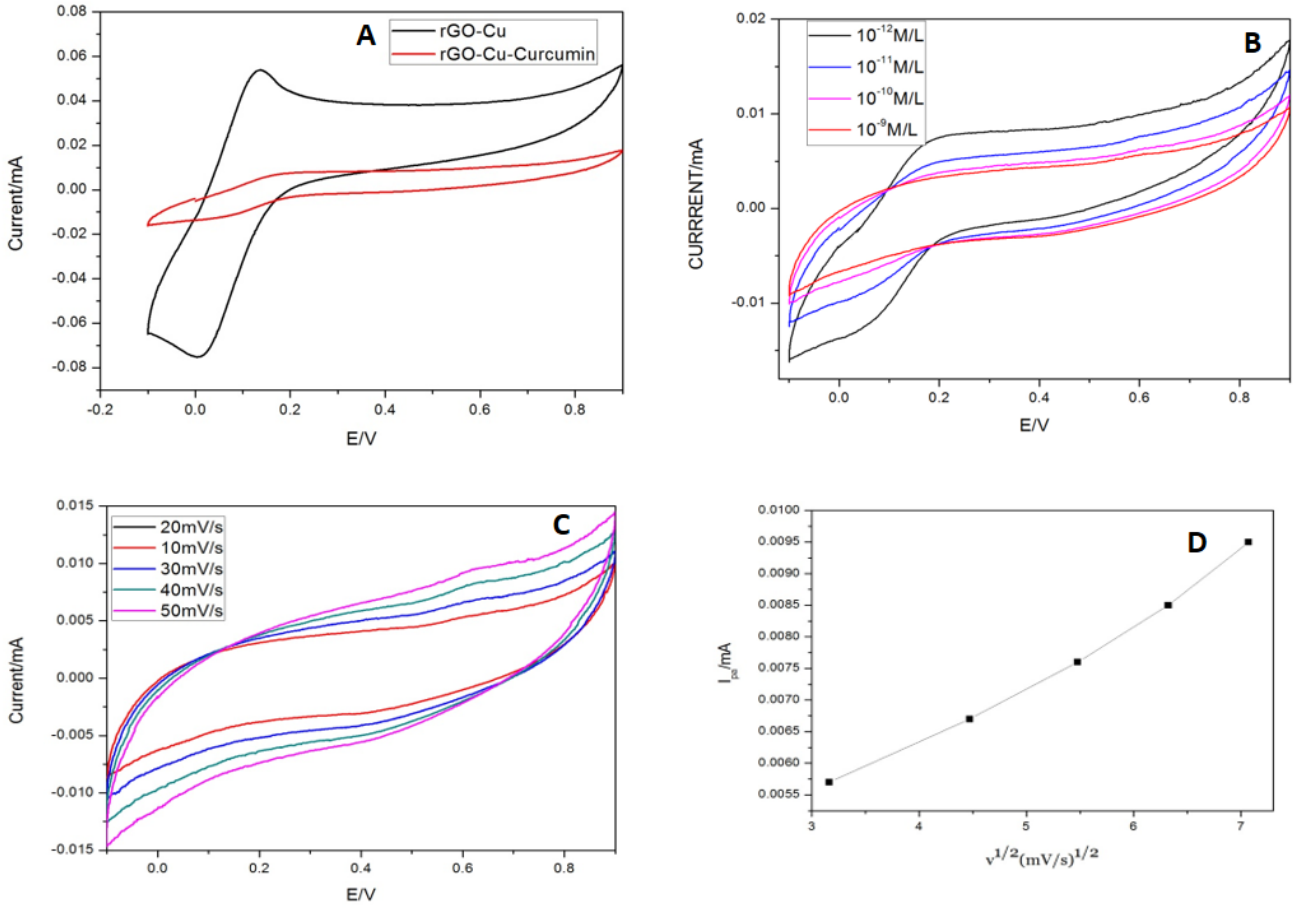

Figure 7. (A) CV studies of Cu-rGO without and with curcumin. (B) CV studies of Cu-rGO with different concentrations of curcumin. (C) CV studies of Cu-rGO at different scans. (D) Linear variation of scan rate for Cu-rGO.

shows oxidation peak also lies in the same range as that of Cu-GO in the supporting electrolyte. When curcumin was added, the oxidation peak was not very profound as that of Cu-GO and also shifted by 0.1V (Figure 7A). At lower concentrations, the copper peak at 0.1 is dominant but as the concentration is increased the curcumin seems to hinder the charge flow at the electrode surface by depositing itself. Hence the curcumin oxidation peak at 0.6V manifests and the 0.1V peak disappears after subsequent runs (Figure 7B). The responses of Cu-GO had better peaks for oxidation and reduction. On the contrary, rGO peaks were so defined. Cu-GO was found to be superior in conductivity of Cu-GO. This makes them potential candidates for sensing application. GO has better binding affinity to copper than rGO because of the presence of more oxygen moieties in the former. And we also have inferred the same from our data. The detection limit of Cu-GO was also found to be better than its other counterpart. The presence of comparatively more oxygen species in GO than rGO leads to better binding of copper and the drug in GO than in rGO. Hence, the mobility of charge is seen more in Cu-GO than in Cu-rGO. The detection limit of the three electrodes showed Cu-GO had 10 times more sensitivity than Cu-rGO electrodes. Repeated casting is required to studies dealing with higher concentration due to enhanced accumulation of the drug. But this will surely show an increase in current as a result of enhanced electroactive species of the drug [58,59].

Sensitivity and detection limit

The detection limit was calculated using 3 sigma rules. The Cu-GO showed a lowest detection of 4.7nM while the Cu-rGO showed a lower detection limit of 0.02nM. Both of these values fall in between the initial linear range for both the electrodes. These values have been the lowest that has been reported for curcumin. The detection limit of copper, Cu-GO and Cu-rGO modified electrodes were found to be 0.006 nM, 4.7nM and 0.02nM respectively.

Analytical applications

Phosphate buffer was used as supporting electrolyte because it mimics physiological fluid conditions. Three fractions of curcumin were introduced in succession into the buffer. The concentrations opted were as per our previously reported work [46]. Cu-GO recovery was found to be 94.22% and for Cu-rGO it was 83.53%. These results substantiate the potential utilization of these sensing materials in plasma samples.

Reusability studies

Both the electrodes were tested in 10-7 M solution of the drug to assess their reproducibility. The study was repeated for 7 cycles for six weeks, the results were found to be good as the change in current was found to be negligible. Hence, it possesses good reproducibility along with good long-term storage application.

Selectivity

Interference species potentially present in the systemic circulation were added along with curcumin to check the change in current density pattern for both the electrode. The species considered were 1mM of sodium, potassium, starch and glucose along with 1mM of Curcumin in the commercial purchased fetal calf serum. The results showed less significant interference by potassium, glucose and starch. Sodium ion was interfering a bit. Drop casted GO or rGO gets rearranged with hydrogen bonds that are strong enough to the individual sheets in a lamellar fashion. The functional groups and water molecules adsorbed on the basal plane and sides of the sheets is the reason behind the large d spacing of these sheets. Studies previously have already proved that sodium ions permeate faster through GO and rGO sheets in comparison to other metals. This penetration also varies with the anion counterpart attached to it ranging from hydroxyl with highest penetration followed by sulphates, chlorides and finally bicarbonates. Since, the sodium ion in our study would have been in hydroxide form in PBS hence these ions penetrated faster in these sheets when compared to curcumin and therefore showing higher sensitivity by spiking the current. The remarkable fact is after these penetrations the sheet conformation stayed intact will only negligible presence of ions in them (<10%). The functional groups in the sheets cause the interlayer distance to be so large to form nanocapillaries which permeates hydrated ions. GO or rGO sheets can be considered as large organic molecule (because of the functional groups) whose interactions with the hydrated ions are responsible for the selective permeation property. Wetted GO/rGO have larger distances between the sheets. Sodium ions are ionic species that should not relatively with the functional groups of the sheets, but the hydroxide form of sodium leads to the reactions between carboxyl and hydroxyl groups in the sheet. This makes GO/rGO sheets chemically active which leads to nanocapillaries to be loser and fast penetration of sodium ions and hence relatively more selective, sensitive and higher conductivity [60].

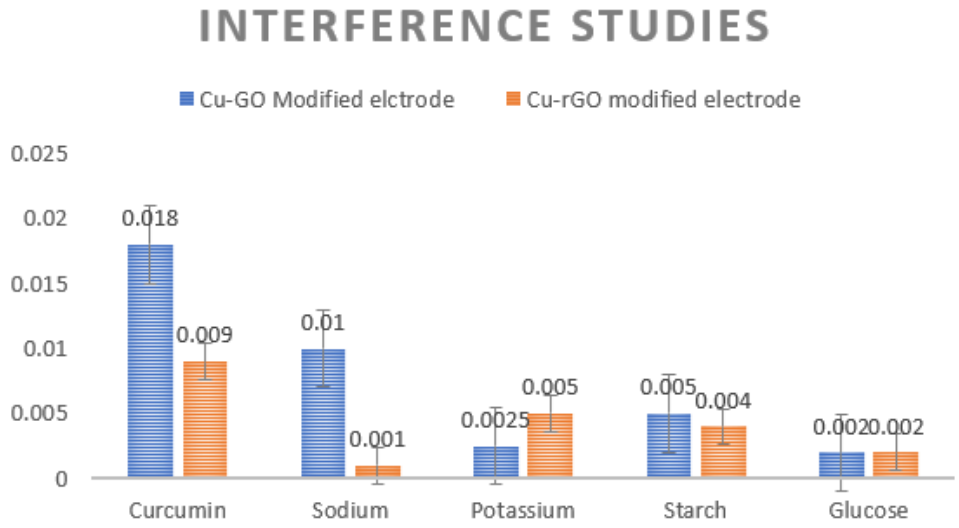

Figure 8. (left to right) Interference studies for Cu-GO and Cu-rGO respectively.

Table 1. Some previously reported curcumin sensors

S.No	Mode	Limit of detection	Year of study	reference
1	CV mode (GO and rGO)	0.2nM	2017	[46]
2	Capacitive Sensing	45x 10^{-6} M	2012	[51]
3	Voltammetry (GCE with graphene)	3 x 10^{-8} mol L^{-1}	2012	[59]
4	Voltammetry (electrochemical rGO)	0.1µM	2012	[59]
5	Spectrophotometry	8 µg mL^{-1}	2009	[61]
6	Fluorescence (HPLC)	0.09 ng mL^{-1}	2010	[62]
7	HPLC (reverse)	100 µg mL^{-1}	2007	[63]
8.	HPLC (CRTO)	-	2002	[64]
9.	Polarography	10^{-8} µM	2010	[65]
10.	Voltammetry (CNT, Dysprosium nanowire)	5.0 x 10^{-10} M	2012	[66]
11.	Voltammetry (GCE)	4.1 × 10^{-6} M	2012	[67]
12.	stripping voltammetry (carbon)	4.9 mM	2012	[68]
13.	Voltammetry (poly- ACBK)	4.1x10^{-8} M	2008	[69]
14	stripping voltammetry (CPE, HMDE)		2011	[70,71]
15	CV (GCE)	0.0416 µM	2014	[71]
16	DPV (GCE)	0.004 µM	2014	[72]
17	ADSV (MWCNT/BPPGE)	0.45 µM	2017	[73]
18	SWV (MWCNT/GCE)	0.89 µM	2017	[74]
19	SWV (Al^{3+}/PdNp/GE)	0.22 µM	2016	[75]
20	SWV (PdNps/Poly(Pr)/GE)	0.001 µM	2014	[76]
21	SWV (NSrGO/Ru@AuNPs/GCE)	2.0 × 10^{-7} µM	2016	[77]
22	DPV (FCNFCPE)	0.02 µM	2016	[78]
23	SWV (CdO-IL/MCPE)	0.08 µM	2016	[79]
24	SWV (NiCl2/GCE)	0.01 µM	2016	[80]
25	Fluorescent–Label free (A nitrogen and phosphorus dual-doped carbon dots)	58 nmol/L	2018	[81]
26	S-55 fluorescence spectrophotometer (Nitrogen-doped fluorescent carbon dots)	29.8 nM	2021	[82]
27.	CV mode (Cu-GO and Cu-rGO)	4.7 nM and 0.02nM	Present study	

Inference pattern is depicted in Figure 8. It exhibits enhanced electrode sensing activity for curcumin and very less effect of the interference species. Glucose and starch are most common compounds present in serum. In addition to the metal nanoparticle the orientation and arrangement of the metal particles onto the GO and rGO matrix contribute for the selective binding of curcumin. The Cu-GO electrode shows good reproducibility and selectivity when compared to its rGO counterpart. The bare copper modified electrode shows lowest detection limit but our current study was to see the effect of GO and rGO with the metal on the detection scenario of our drug. Table 1 reports the various sensors that have been attempted to detect curcumin [46,51,58-82]. Not all previous experiments were done with similar units, modes and parameters hence a column for linear range and pH which might cause confusion for the reader. Detection limit is the main aspect for a biosensor hence the detection limit has been compared.

Proposed mechanism of reaction

Our target compound forms complexes in the presence of 1,3 diketone with metal ions. The tautomerism caused by the ligand's keto-enol groups are the reason behind this interaction. As an electrode modified this copper complex of curcumin can electron transfer heterogeneously through the inner sphere. The major mechanism behind this interaction would be the hydroxyl group at the 4th position of the phenyl ring's gets blocked. The centralized metal ion (copper (II)) coordinates with curcumin by cheating in the square planar geometry of coordination. The ligands are found to be almost planar as there is an extensive π-π stacking in two-way orientation to the adjacent ligands. Hence, the reaction between the target and copper is mainly due to π- π conjugated system of large magnitude (electron transfer system). While rGO interacts with the aliphatic and aromatic groups of curcumin via π-π stacking.

Conclusion

In the present study a new type of electrode material combination was experimented. The studies of cyclic voltammtery on copper alone, followed by its combination with graphene oxide ad reduced graphene oxide were studied successfully. The ranges were found to be linear at different concentrations for each of the combination. For copper decorated electrode the detection limit was found to be 0.006 nM, whereas for Cu-GO 4.7nM and for Cu-rGO 0.02nM. the difference in the oxygen concentration and functional groups for reaction might be the possible reason behind the variation in the ranges in detection. they had good specificity and were reproducible to a good extend. Although bare metal shows better detection limit incorporation in GO and rGO gives new light on how these carbon materials can be used in enhanced fashion for detection. these were very good examples for non- enzymatic sensing of analytes in quantities similar to the ones existing in the systemic circulation.

V Future Scope

The future scope of the work would be to find potential materials that would aid in analysing our target with even more efficacy. These kinds of electrochemical assay can be used to find many aspiring and suitable combinations of compounds that would revolutionize the food and pharmaceutical market.

Acknowledgements

The grant was provided by Department of Science and Technology under DST- INSPIRE fellowship. The grant number is IF150627.

Competing interests

The Authors have no competing interests to declare.

References

1. Abbaspouar A, Ghaffarinejad A (2011) Copper Oxide Nanoparticle Modified Sol–Gel-Derived Carbon Ceramic by Microwave Irradiation, and Its Application for Determination of Adenine at Very Low Potential. *Electroanalysis* 23: 651.
2. Afzali M, Mostafavi A, Shamspur T (2016) Electrospun composite nanofibers of poly vinyl pyrrolidone and zinc oxide nanoparticles modified carbon paste electrode for electrochemical detection of curcumin. *Mater Sci Eng: C* 68: 789-797. [Crossref]
3. Alexander S, Baraneedharan P, Balasubrahmanyan S, Ramaprabhu S (2017) Modified graphene based molecular imprinted polymer for electrochemical non-enzymatic cholesterol biosensor. *European Polymer Journal* 86: 106-116.
4. An Z, Li J, Kikuchi A, Wang Z, Jiang Y, et al. (2019) Mechanically strengthened graphene-Cu composite with reduced thermal expansion towards interconnect applications. *Microsystems & Nanoengineering* 5: 20
5. Anand P, Kunnumakkara AB, Aggarwal BB (2007) Bioavailability of curcumin: problems and promises. *Mol Pharm* 4: 807-818. [Crossref]
6. Appiah-Opong R, Commandeur JN, Vugt-Lussenburg B, Vermeulen NP (2007) Inhibition of human recombinant cytochrome P450s by curcumin and curcumin decomposition products. *Toxicol* 235: 83-91. [Crossref]
7. Arslan E, Çakır S (2014) A novel palladium nanoparticles-polyproline-modified graphite electrode and its application for determination of curcumin. *J Solid State Electrochem* 18: 1611-1620.
8. Asai A, Miyazawa T (2000) Occurrence of orally administered curcuminoid as glucuronide and glucuronide/sulfate conjugates in rat plasma. *Life Sci* 67: 2785-2793. [Crossref]
9. Atal CK, Dubey RK, Singh, J (1985) Biochemical basis of enhanced drug bioavailability by piperine: evidence that piperine is a potent inhibitor of drug metabolism. *J Pharmacol Exp Ther* 232: 258-262. [Crossref]
10. Baia S, Shen X (2012) Graphene–inorganic nanocomposites. *RSC Adv* 2: 64-98
11. Barik A, Mishraa B, Shen L, Mohan H, Kadam RM, et al. (2005) Evaluation of a new copper(II)-curcumin complex as superoxide dismutase mimic and its free radical reactions. Free Radical Bio Med 39: 811-822.
12. Baum L, Ng A (2004) Curcumin interaction with copper and iron suggests one possible mechanism of action in Alzheimer's disease animal models. J Alzheimer's Dis 6: 367-377. [Crossref]
13. Çakır S, Biçer E Arslan EY (2015) A Newly Developed Electrocatalytic Oxidation and Voltammetric Determination of Curcumin at the Surface of PdNp-graphite Electrode by an Aqueous Solution Process with Al3+Croat. *Chem Acta* 88: 105-112.
14. Chaisiwamongkhol K, Ngamchuea K, Batchelor-McAuley C, Compton RG (2017) Multiwalled Carbon Nanotube Modified Electrodes for the Adsorptive Stripping Voltammetric Determination and Quantification of Curcumin in Turmeric. *Electroanalysis* 29: 1049-1055.
15. Chan WH, Wu HY, Chang WH (2006) Dosage effects of curcumin on cell death types in a human osteoblast cell line. *Food Chem Toxicol* 44: 1362-1371. [Crossref]
16. Cheng Q, Tang J, Ma J, Zhang H, Shinya N, et al. (2011) Graphene and carbon nanotube composite electrodes for supercapacitors with ultra-high energy density. *Phys Chem* 13: 17615.
17. Cheraghi S, Taher MA, Karimi-Maleh H (2016) Fabrication of Fast and Sensitive Nanostructure Voltammetric Sensor for Determination of Curcumin in the Presence of Vitamin B9 in Food Samples. *Electroanalysis* 28: 2590-2597.
18. Cortéıs JS, ranados SG, Ordaz AA, Jime´ınez JAL, Griveau S, et al. (2007) Electropolymerized manganese tetraaminophthalocyanine thin films onto platinum ultramicroelectrode for the electrochemical detection of peroxynitrite in solution. *Electroanalysis* 19: 61-64.
19. Daneshga P, Norouzi P, Movahedi AAM, Ganjali MR, Haghshenas E, et al. (2009) Fabrication of carbon nanotube and dysprosium nanowire modified electrodes as a sensor for determination of curcumin. *J Applied Electrochem* 39: 1983
20. Dey N, Devasena T, Ramaprabhu S, Francis AP (2016) Validation of First Generation Dry Capacitive Sensing System for the Detection of Curcumin. *Sensor Lett* 14: 710-718.
21. Dey N, Devasena T, Sivalingam T (2017) A Comparative evaluation of Graphene oxide-based materials for Electrochemical non-enzymatic sensing of Curcumin. *Mater Res Express* 5.
22. Fan ZJ, Wang K, Wei T, Yan J, Song LP, Shao B (2010) An environmentally friendly and efficient route for the reduction of graphene oxide by aluminum powder. *Carbon* 48: 1670-1692.
23. Ghalebani, L, Wahlström A, Danielsson J, Wärmländer SK, Gräslund A (2012) pH-dependence of the specific binding of Cu(II) and Zn(II) ions to the amyloid-β peptide'. *Biochem Biophys Res Communicat* 421: 554-560. [Crossref]
24. Gholivand MB, Ahmadi F, Pourhossein A (2011) Adsorptive cathodic stripping voltammetric determination of curcumin in turmeric and human serum, Czech. *Chem Commun* 76: 143- 157.
25. Goel A, Kunnumakkara AB, Aggarwal BB (2009) Curcumin as "Curecumin": from kitchen to clinic. *Biochem Pharmacol* 75: 787-809. [Crossref]
26. Gong YLXJ, Dong W, Zhou RX, Shuang S, Dong C (2018) Nitrogen and phosphorus dual-doped carbon dots as a label-free sensor for Curcumin determination in real sample and cellular imaging. *Talanta* 183: 61-69.
27. He H, Gao C (2010) Supraparamagnetic, Conductive, and Processable Multifunctional Graphene Nanosheets Coated with High-Density Fe3O4 Nanoparticles. *ACS Appl Mater Interfaces* 2: 3201. [Crossref]
28. Ireson CR, Jones DJ, Orr S, Coughtrie MW, Boocock DJ, et al. (2002) Metabolism of the cancer chemopreventive agent curcumin in human and rat intestine. *Cancer Epidemiol Biomarkers Prev* 11: 105-111. [Crossref]
29. Jadhav BK, Mahadik KR, Paradkar AR (2007) Development and validation of improved reversed phase-HPLC method for simultaneous determination of curcumin, demethoxycurcumin and bis-demethoxycurcumin. *Chromatographia* 65: 483-488
30. Jain R, Haque A, Verma AJ (2017) Voltammetric quantification of surfactant stabilized curcumin at MWCNT/GCE sensor. *Mol Liq* 230: 600-607.
31. Jayaprakasha GK, Rao LJM, Sakaria KK (2002) Improved HPLC method for the determination of curcumin, demethoxycurcumin, and bisdemethoxycurcumin. *J Agri Food Chem* 50: 3668-3672. [Crossref]
32. Jiang T, Zhou GR, Zhang YH, Sun PC, Du QM, et al. (2012) Influence of curcumin on the Al(III)-induced conformation transition of silk fibroin and resulting potential therapy for neurodegenerative diseases. *RSC Advances* 2: 9106-9113.
33. Kotan G, Kardaş F, Yokuş OA, Akyıldırım O, Saral H, et al. (2016) A novel determination of curcumin via Ru@Au nanoparticle decorated nitrogen and sulfur-functionalized reduced graphene oxide nanomaterials. *Anal Methods* 8: 401-408.
34. Kovtyukhova NI, Ollivier PJ, Martin BR, Mallouk TE, Chizhik SA, et al. (1999) Layer-by-Layer Assembly of Ultrathin Composite Films from Micron-Sized Graphite Oxide Sheets and Polycations. *Chem Mater* 11: 771.
35. Kunnumakkara AP, Sundaram C, Harikumar KB, Tharakan ST, Lai OS, et al. (2008) Cancer is a preventable disease that requires major lifestyle changes. *Biochem Pharmacol* 76: 1590-1611. [Crossref]
36. Li B, Cao H, Yin G, Lu Y, Yin J (2011) Cu2O@reduced graphene oxide composite for removal of contaminants from water and supercapacitors. *J Mater Chem* 21: 10645
37. Li K, Li Y, Yang L, Wang L, Ye B (2014) The electrochemical characterization of curcumin and its selective detection in Curcuma using a graphene-modified electrode. *Analytical Chem* 6: 7801-7808.
38. Lian P, Zhu X, Xiang HF, Li Z, Wang H (2010) Enhanced cycling performance of Fe3O4–graphene nanocomposite as an anode material for lithium-ion batteries. *Electrochim Acta* 56: 834.
39. Liang J, Xu Y, Sui D, Zhang L, Huang Y, et al. (2010) Flexible, Magnetic, and Electrically Conductive Graphene/Fe3O4 Paper and Its Application for Magnetic-Controlled Switches. *J Phys Chem C* 114: 17465.
40. Liu CJ, Zhang P, Tian F, Li W, Lib F, et al. (2011) One-step synthesis of surface passivated carbon nanodots by microwave assisted pyrolysis for enhanced multicolor photoluminescence and bioimaging. *J Mater Chem* 21: 13765.
41. Long Y, Zhang W, Wang F, Chen Z (2014) Simultaneous determination of three curcuminoids in Curcuma longa L. by high performance liquid chromatography coupled with electrochemical detection. *J Pharm Anal* 4: 325-330.

42. Lorenz WS, Subhan VA, Edelmann FT (2015) Metal complexes of curcumin - synthetic strategies, structures and medicinal applications. *Chem Society Rev* 44: 4986-5002. [Crossref]

43. Mancuso C, Barone E (2009) Curcumin in clinical practice: myth or reality? *Trends in Pharmacol Sci* 30: 333-334. [Crossref]

44. Mashazi P, Togo C, Limson J, Nyokong T (2010) Applications of polymerized metal tetra-amino phthalocyanines towards hydrogen peroxide detection. *J Porphyrins Phthalocyanines* 14: 252-263.

45. Mawani Y, Orvig C (2014) Improved separation of the curcuminoids, syntheses of their rare earth complexes, and studies of potential antiosteoporotic activity. *J Inorg Biochem* 132: 52-58. [Crossref]

46. Miao XM, Yuan R, Chai YQ, Shi YT, Yuan YY (2008) Direct electrocatalytic reduction of hydrogen peroxide based on Nafion and copper oxide nanoparticles modified Pt electrode. *J Electroanal Chem* 612: 157

47. Modi G, Pitre KS (2010) Electrochemical Analysis of Natural Chemopreventive Agent (Curcumin) in Extracted Sample and Pharmaceutical Formulation. *Defence Sci J* 60: 255-258.

48. Moniri S, Ghoranneviss M, Hantehzadeh MR, Asadabad MA (2017) Synthesis and optical characterization of copper nanoparticles prepared by laser ablation. *Bulletin Mater Sci* 40: 37-43.

49. Obirai J, Nyokong T (2004) Electrochemical studies of manganese tetraamminophthalocyanine monomer and polymer. *Electrochim Acta* 49: 1417-1428.

50. Pan MH, Huang TM, Lin JK (1999) Biotransformation of curcumin through reduction and glucuronidation in mice. *Drug Metabolism and Disposition* 27: 486-494. [Crossref]

51. Peng J, Nong K, Cen L (2012) Electropolymerization of Acid Chrome Blue K on Glassy Carbon Electrode for the Determination of Curcumin. *J Chinese Chem Soc* 59: 1415-1420.

52. Pundarikakshudu K, Dave HN (2009) Simultaneous determination of curcumin and berberine in their pure form and from the combined extracts of curcuma longa and Berberis aristate. *Int J Applied Sci Eng* 8: 19-26.

53. Qin J, Cao M, Lia N and Hu C (2011) Graphene-wrapped WO3 nanoparticles with improved performances in electrical conductivity and gas sensing properties. *J Mater Chem* 21: 17167.

54. Selvakumar D, Sivaram H, Alsalme A, Jayavel R (2016) Facile synthesize of free standing highly conducting flexible reduced graphene oxide. *J Mater Sci Mater Electron* 27: 6232-6241.

55. Song H, Zhang L, He C, Qu Y, Tiana Y, et al. (2011) Graphene sheets decorated with SnO2nanoparticles: in situ synthesis and highly efficient materials for cataluminescence gas sensors. *J Mater Chem* 21: 5972.

56. Stanić Z, Voulgaropoulos A, Girousi S (2008) Electroanalytical Study of the Antioxidant and Antitumor Agent Curcumin. *Electroanalysis* 20: 1263-1266.

57. Sudibyo OS, Commandeur M, Samhoedi JNR, Vermeulen NP (1996) Effects of curcumin on cytochrome P450 and glutathione S-transferase activities in rat liver. *Biochem Pharmacol* 51: 39-45. [Crossref]

58. Sun X, Liu Z, Welsher K, Robinson JT, Goodwin A, et al. (2008) Nanographene oxide for cellular imaging and drug delivery. *Nano Res* 1: 203-212. [Crossref]

59. Tanga X, Yua H, Buib B, Wang L, Xing C, et al. (2021) Nitrogen-doped fluorescence carbon dots as multi-mechanism detection for iodide and curcumin in biological and food samples. *Bioactive Mater* 6: 1541-1554

60. Umar A, Rahman MM, Hajry A, Hahn YB (2009) Enzymatic Glucose Biosensor Based on Flower-Shaped Copper Oxide Nanostructures Composed of Thin Nanosheets. *Electrochem Commun* 11: 278

61. Vareed SK, Kakarala M, Ruffin MT, Crowell JA, Normolle DP, et al. (2008) Cancer Epidemiology. *Biomarkers and Prevention* 17: 1411-1417.

62. Wang H, Robinson JT, Diankov G, Dai H (2010) Nanocrystal Growth on Graphene with Various Degrees of Oxidation. *J Am Chem Soc* 132: 3270.

63. Wang X, Song L, Yang H, Xing W, Luac H, et al. (2012) Cobalt oxide/graphene composite for highly efficient CO oxidation and its application in reducing the fire hazards of aliphatic polyesters. *J Mater Chem* 22: 3426.

64. Waranyoupalin R, Wongnawa S, Wongnawa M, Pakawatchai C, Panichayupakaranant P, et al. (2009) Studies on complex formation between curcumin and Hg(II) ion by spectrophotometric method: A new approach to overcome peak overlap. *Cent Eur J Chem* 7: 388-394.

65. Wilkinson JY, Wang JDX, Hatcher W, Kock H, D'Agostino ND Jr, et al. (2009) Curcumin, a cancer chemopreventive and chemotherapeutic agent, is a biologically active iron chelator. *Blood* 113: 462-469. [Crossref]

66. Willander M, Hasan KU, Nur O, Zainelabdin A, Zamana S, et al. (2011) Recent progress on growth and device development of ZnO and CuO nanostructures and graphenenanosheets. *J Mater Chem* 22: 2337.

67. Wilson NR, Pandey PA, Young RBRJ, Kinloch IA, Gong L, et al. (2009) Graphene Oxide: Structural Analysis and Application as a Highly Transparent Support for Electron Microscopy. *ACS Nano* 3: 2547. [Crossref]

68. Wray DM, McAuley CB, Compton RG (2012) Compton RG, Selective Curcuminoid Separation and Detection via Nickel Complexation and Adsorptive Stripping Voltammetry. *Electroanalysis* 24: 2244-2248.

69. Wu L, Tsui LK, Swami N, Zangari G (2010) Photoelectrochemical Stability of Electrodeposited Cu2O Films. *J Phys Chem C* 114: 11551-11556.

70. Xue Y, Chen H, Yu D, Wang S, Yardeni M, et al. (2011) Oxidizing metal ions with graphene oxide: the in situ formation of magnetic nanoparticles on self-reduced graphene sheets for multifunctional applications. *Chem Commun* 47: 11689.

71. Yallapu MM, Jaggi M, Chauhan SC (2012) Curcumin nanoformulations: a future nanomedicine for cancer. *Drug Discovery Today* 17: 71-80. [Crossref]

72. Yan XY, Tong XL, Zhang YF, Han XD, Wang YY, et al. (2012) Cuprous dispersed on reduced graphene oxide as an efficient electrocatalyst for oxygen reduction reaction. *Chem Commun* 48: 1892.

73. Yang H, Wang YLMJJ, Fu H (2011) General Copper-Catalyzed Transformations of Functional Groups from Arylboronic Acids in Water. *Chem Eur J* 17: 5652.

74. Yang S, Feng X, Ivanovici S, Müllen K (2010) Fabrication of Graphene-Encapsulated Oxide Nanoparticles: Towards High-Performance Anode Materials for Lithium Storage. *Angew Chem Int Ed* 49: 8408. [Crossref]

75. Yoon T, Chae C, Sun YK, Zhao X, Kung HH, et al. (2011) Bottom-up in situ formation of Fe3O4nanocrystals in a porous carbon foam for lithium-ion battery anodes. *J Mater Chem* 21: 17325.

76. Zhang J, Yang H, Shen G, Cheng P, Zhang P, et al. (2010) Reduction of graphene oxide via L-ascorbic acid. *Chem Commun* 46: 1112-1114. [Crossref]

77. Zhang X, Sui Z, Xu B, Yue S, Luo Y, et al. (2011) Mechanically strong and highly conductive graphene aerogel and its use as electrodes for electrochemical power sources. *J Mater Chem* 21: 1673.

78. Zhang Z, Li X, Wang C, Zhang C, Liu P, et al. (2012) A novel dinuclear Schiff-base copper (II) complex modified electrode for Ascorbic acid catalytic oxidation and determination. *Dalton Transactions* 41: 1252-1258.

79. Zhao L, Chen F, Zhao G, Wang Z, Liao X, et al. (2005) Isomerization of trans-astaxanthin induced by copper(II) ion in ethanol. *J Agri Food Chem* 53: 9620-9623. [Crossref]

80. Zhou G, Wang DW, Li F, Zhang L, Li N, et al. (2010) Graphene-Wrapped Fe3O4 Anode Material with Improved Reversible Capacity and Cyclic Stability for Lithium Ion Batteries. *Chem Mater* 22: 5306.

81. Ziyatdinova GK, Nizamova AM, Budnikov HC (2012) Voltammetric determination of curcumin in spices. *J Analyt Chem* 67: 591-594.

82. Zokhtareh R, Rahimnejad M (2018) A Novel Sensitive Electrochemical Sensor Based on Nickel Chloride Solution Modified Glassy Carbon Electrode for Curcumin Determination. *Electroanalysis* 30: 921-927.